Ultrafast Photoswitched Charge Transmission through the Bridge Molecule in a Donor−Bridge−Acceptor System

Ryan T. Hayes,[†] Michael R. Wasielewski,*[,†] and David Gosztola[‡]

Contribution from the Department of Chemistry, Northwestern University, Evanston, Illinois 60208-3113, and the Chemistry Division, Argonne National Laboratory, Argonne, Illinois 60439-4831

Received January 20, 2000

Abstract: A Donor−Bridge−Acceptor molecule, D−B−A, was synthesized to probe the effects of changing the electronic state of the bridge molecule, B, on the rates of electron transfer within D−B−A. Selective photoexcitation of D in a tetrahydrofuran solution of D−B−A with 400 nm, 130 fs laser pulses at $t = 0$ ps results in photoinduced electron transfer to yield the ion pair D^+-B^-A with $\tau = 60$ ps, which undergoes a subsequent charge shift with $\tau = 140$ ps to yield the long-lived ion pair D^+-B-A^- ($\tau = 700$ ns). Subsequent selective photoexcitation of B within D^+-B-A^- with a 520 nm, 150 fs laser pulse at $t = 500$ ps results in about 20% of the D^+-B-A^- population undergoing charge recombination with $\tau = 100$ ps. This charge recombination rate is about 7000 times faster than the normal recombination rate of the ion pair. The results demonstrate that formation of the lowest excited singlet state of the bridge molecule B significantly alters the reaction pathways leading to charge recombination. Thus, D−B−A can be viewed as a molecular switch in which the D^+-B-A^- state can be rapidly turned on and off using 400 and 520 nm laser pulses, respectively.

Introduction

The rates and mechanisms of electron and hole transfer through organic molecules are topics of considerable recent interest.[1,2] One aspect of this interest is the question of whether single molecules can act as molecular wires.[3−10] In addition, as the limits of current silicon-based technologies in electronics are approached,[11] a related question is whether molecular systems can be used as electronic components such as ultrafast switches.[12,13] Central to both of these issues is the question of how to control charge transmission through organic molecules. We have developed three fundamental approaches to exerting such control over electron-transfer pathways.

One of these strategies uses photoinduced electron transfer to produce a radical ion pair in the donor−acceptor array: $D^+-A_1^--A_2$. The reduced acceptor A_1^- possesses an intense optical absorption that can be irradiated with a second laser pulse to produce the excited-state $D^+-{}^1{*}A_1^--A_2$ that is capable of transferring an electron to the secondary acceptor A_2. We have already demonstrated that sequential application of femtosecond laser pulses to both linear and branched systems of this type can propagate the electron up a potential gradient in the linear case,[14] and result in an optically controlled change of electron transport direction in the branched case.[15] The second approach recognizes that the rates of electron-transfer reactions can be controlled through the application of electric fields. A considerable amount of work has been devoted to the theoretical modeling[16−18] and experimental realization[19−21] of molecular electronic switches consisting of organic electron donor−acceptor pairs whose operation is controlled by an external electric field. The electric field produced by a photogenerated ion pair can have a large effect on the electronic states of surrounding molecules. For example, a photogenerated electric field can affect the optical properties of a nearby molecule, or even alter the rate of electron transfer between a second donor−acceptor pair. If each of these processes is photodriven, logic can be developed based on the number, sequence, and frequencies of optical pulses used to produce a particular optical observable in these systems. We have prepared two $donor_1-acceptor_1-acceptor_2-donor_2$ molecular arrays, $D_1-A_1-A_2-D_2$,[22,23] in which photoinduced

* Address correspondence to this author. E-mail at wasielew@chem.nwu.edu.

† Northwestern University.

‡ Argonne National Laboratory.

(1) Bixon, M.; Jortner, J. *J. Chem. Phys.* **1997**, *107*, 5154−5170.

(2) Jortner, J.; Bixon, M. Electron Transfer−From Isolated Molecules to Biomolecules, Parts 1 and 2. In *Adv. Chem. Phys.* **1999**, *106*.

(3) Bissell, R. A.; Cordova, E.; Kaifer, A. E.; Stoddart, J. F. *Nature* **1994**, *369*, 133−137.

(4) Bumm, L. A.; Arnold, J. J.; Cygan, M. T.; Dunbar, T. D.; Burgin, T. P.; Jones, L., II; Allara, D. L.; Tour, J. M.; Weiss, P. S. *Science (Washington, D.C.)* **1996**, *271*, 1705−07.

(5) Andres, R. P.; Bein, T.; Dorogi, M.; Feng, S.; Henderson, J. I.; Kubiak, C. P.; Mahoney, W.; Osifchin, R. G.; Reifenberger, R. *Science (Washington, D. C.)* **1996**, *272*, 1323−1325.

(6) Tsivgoulis, G. M.; Lehn, J. M. *Adv. Mater. (Weinheim, Ger.)* **1997**, *9*, 39−42.

(7) Davis, W. B.; Wasielewski, M. R.; Ratner, M. A.; Mujica, V.; Nitzan, A. *J. Phys. Chem. A* **1997**, *101*, 6158−6164.

(8) Davis, W. B.; Svec, W. A.; Ratner, M. A.; Wasielewski, M. R. *Nature (London)* **1998**, *396*, 60−63.

(9) Schlicke, B.; Belser, P.; De Cola, L.; Sabbioni, E.; Balzani, V. *J. Am. Chem. Soc.* **1999**, *121*, 4207−4214.

(10) Chen, J.; Reed, M. A.; Rawlett, A. M.; Tour, J. M. *Science (Washington, D.C.)* **1999**, *286*, 1550−1552.

(11) Packan, P. A. *Science* **1999**, *285*, 2079−2081.

(12) Jortner, J.; Ratner, M., Eds. *Chemistry for the 21st Century*, Monograph; Oxford: Malden, MA, 1997.

(13) de Silva, A. P.; Gunaratne, H. Q. N.; Gunnlaugsson, T.; Huxley, A. J. M.; McCoy, C. P.; Rademacher, J. T.; Rice, T. E. *Chem. Rev.* **1997**, *97*, 1515.

(14) Debreczeny, M. P.; Svec, W. A.; Marsh, E. M.; Wasielewski, M. R. *J. Am. Chem. Soc.* **1996**, *118*, 8174−8175.

(15) Lukas, A. S.; Miller, S. E.; Wasielewski, M. R. *J. Phys. Chem. B* **2000**, *104*, 931−940.

(16) Aviram, A.; Ratner, M. A. *Chem. Phys. Lett.* **1974**, *29*, 277−83.

(17) Aviram, A.; Joachim, C.; Pomerantz, M. *Chem. Phys. Lett.* **1988**, *146*, 490−5.

(18) Broo, A. *NATO ASI Ser., Ser. E* **1993**, *240*, 163−75.

(19) Garnier, F.; Horowitz, G.; Peng, X.; Fichou, D. *Adv. Mater. (Weinheim, Fed. Rep. Ger.)* **1990**, *2*, 592−4.

(20) Sambles, J. R.; Martin, A. S. *Phys. Scr., T* **1993**, *T49B*, 718−20.

(21) Tour, J. M.; Wu, R. Report "Extension of branches for orthogonally fused molecular switches", Department of Chemistry, University of South Carolina, Columbia, SC, 1991.

(22) Debreczeny, M. P.; Svec, W. A.; Wasielewski, M. R. *Science (Washington, D.C.)* **1996**, *274*, 584−587.

10.1021/ja000219d CCC: $19.00
Published on Web 05/23/2000

charge separation within one donor−acceptor pair controls the rate constants for photoinduced charge separation and thermal charge recombination within a second donor−acceptor pair. In the latter case, photoinduced production of either $D_1^+-A_1^--A_2-D_2$ or $D_1-A_1-A_2^--D_2^+$ completely inhibits formation of the second ion pair following absorption of a second laser pulse. The controlled movement of electrons and/or holes within these organic molecules can be used to develop logical operations as well as information storage applications.

In this paper we demonstrate a third strategy in which charge transmission through the bridging molecule B within a Donor−Bridge−Acceptor (D−B−A) molecule can be optically controlled by selective photoexcitation of B, thus creating a new type of molecular switch that depends on altering the electronic state of B. We have synthesized the D−B−A molecule illustrated below and have observed that selective photoexcitation of D results in the reaction sequence ^{1}*D−B−A → D$^+$−B$^-$−A → D$^+$−B−A$^-$. The intermediate electron carrier B is also a chromophore that can be selectively photoexcited within D$^+$−B−A$^-$ to produce D$^+$−^{1}*B−A$^-$ in which the reaction pathways leading to charge recombination are significantly altered. This results in a reaction rate for charge recombination that is nearly 7000 times more rapid than that observed for D$^+$−B−A$^-$.

Results and Discussion

The donor−bridge−acceptor molecule, D−B−A, is composed of three electronically distinct subunits, D = zinc 5-phenyl-10,15,20-tri(*n*-pentyl)porphyrin, B = perylene-3,4-dicarboximide, and A = 1,8:4,5-naphthalenediimide. To characterize the spectroscopy and electron-transfer reactions of D−B−A, the model compounds D−B, B−A, and B′−A, where B′ does not possess the phenyl group between B and A, as well as the individual species D, B, and A were also studied. The structures of these molecules are shown below, while the syntheses of the molecules used in this study are described in the Supporting Information. The NMR and mass spectra of these molecules are consistent with their assigned structures. The ground-state optical absorption spectrum of D−B−A as well as those of D, B, and A are shown in Figure 1. The data reveal that the spectrum of D−B−A can be closely approximated by a sum of the spectra of D, B, and A. The lowest excited singlet state energies of D, B, and A were each determined from the average of the lowest energy transition in their absorption spectra and the highest energy transition in their fluorescence emission spectra. The absorption maxima of the lowest energy electronic transitions within D, B, and A are 602, 517, and 380 nm, respectively, while the corresponding emission maxima for D, B, and A are 606, 555, and 398 nm, respectively. These data yield lowest excited singlet state energies of 2.06, 2.32, and 3.20 eV, for D, B, and A, respectively.

At 400 nm, the laser wavelength used to generate D$^+$−B−A$^-$ in the time-resolved experiments described below, the Soret band absorbance of the zinc porphyrin donor is about 3.5 times larger than that of the perylene-3,4-dicarboximide chromophore, and is about 10 times larger than that of the 1,8:4,5-naphthalenediimide acceptor. Excitation of the Soret band in D results in subpicosecond internal conversion leading to the low-lying ^{1}*D state. In addition, since ^{1}*D is the lowest excited singlet state within D−B−A, excitation of a small fraction of either B or A within D−B−A with 400 nm light results in subpicosecond energy transfer to form ^{1}*D−B−A (*vide infra*).

(23) Gosztola, D.; Niemczyk, M. P.; Wasielewski, M. R. *J. Am. Chem. Soc.* **1998**, *120*, 5118−5119.

Chart 1

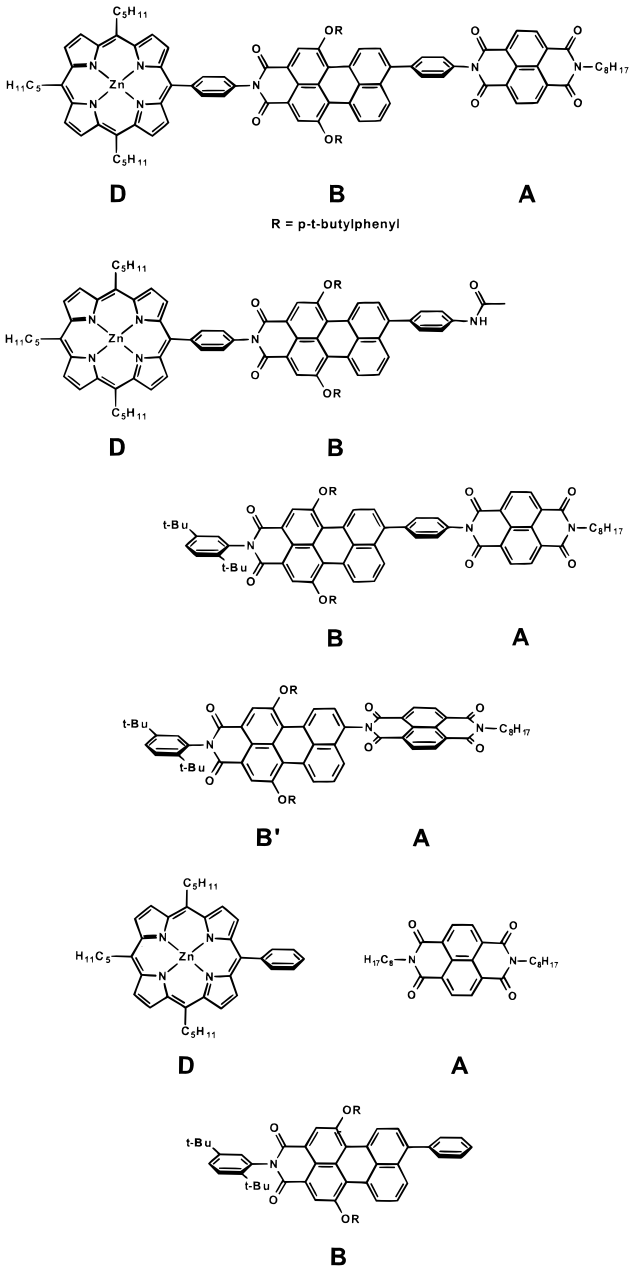

The energy levels of the D$^+$−B$^-$−A and D$^+$−B−A$^-$ ion pairs in tetrahydrofuran were determined from the sum of the one-electron redox potentials for formation of the individual ions in butyronitrile corrected for Coulombic interactions and ion solvation energy differences between the two solvents using the Weller equation:[24]

$$\Delta G_{IP} = E_{OX} - E_{RED} - \frac{e^2}{r_{DA}\cdot\epsilon_S} + e^2\left(\frac{1}{2r_D} + \frac{1}{2r_A}\right)\left(\frac{1}{\epsilon_S} - \frac{1}{\epsilon_{sp}}\right) \quad (1)$$

The accuracy of this treatment is reasonable for solvents of moderate polarity, such as THF.[25] The one-electron oxidation potentials of D and B are 0.65 and 1.40 V, respectively, while the one-electron reduction potentials of B and A are −0.90 and −0.53V, respectively (all vs SCE in butyronitrile), $\epsilon_S = 6.9$ for

(24) Greenfield, S. R.; Svec, W. A.; Gosztola, D.; Wasielewski, M. R. *J. Am. Chem. Soc.* **1996**, *118*, 6767−6777.

(25) Weller, A. *Z. Phys. Chem.* **1982**, *133*, 93−98.

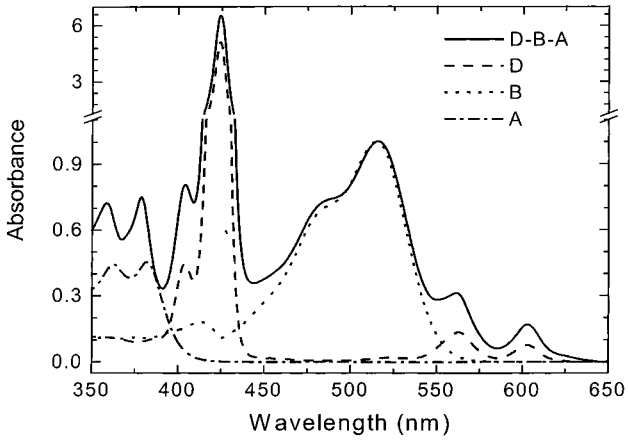

Figure 1. Ground-state absorption spectra of the individual chromophores and D−B−A.

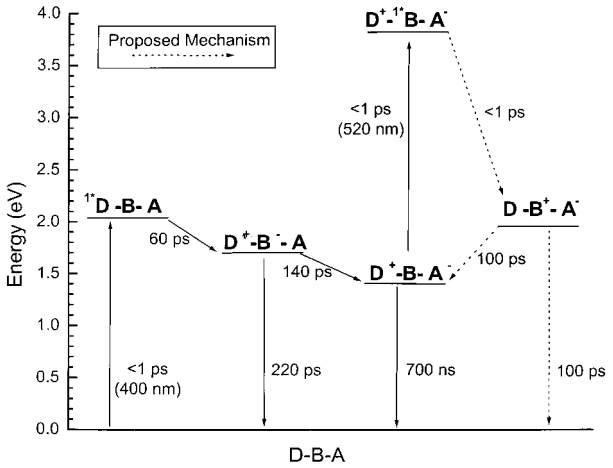

Figure 2. Energy level diagram for D−B−A in tetrahydrofuran.

THF and $\epsilon_{sp} = 25$ for butyronitrile, $r_D = 5$ Å, $r_A = 4$ Å, $r_{DB} = 14.3$ Å, and $r_{DA} = 26.7$ Å.[26] Using these data the ion pair energies of D^+-B^--A and D^+-B-A^- calculated using eq 1 are approximately 1.7 and 1.4 eV, respectively, so that, ΔG_{CS} for charge separation is about −0.4 eV for ^{1}*D−B−A → D^+-B^--A and −0.3 eV for $D^+-B^--A \rightarrow D^+-B-A^-$, Figure 2.

One and two pump pulse transient absorption spectra and kinetics of D−B−A and the reference dyads were measured in THF using an amplified Ti:sapphire laser system, which provides a 130 fs, 400 nm, 2 μJ pump pulse as well as a second, 520 nm, 150 fs, 1 μJ pump pulse along with a white light continuum probe pulse as described earlier.[15,23] Selective single-pump excitation of the porphyrin donor, D, at 400 nm in both D−B−A and D−B results in electron transfer from ^{1}*D to B with $\tau = 60$ ps to yield D^+-B^--A and D^+-B^-, respectively, as indicated by the optical spectrum of B^-, which exhibits a peak near 620 nm, Figure 3.[27] Following excitation, the Q-bands of D at 560 and 602 nm bleach with $\tau < 1$ ps, which indicates that the formation of ^{1}*D either by direct excitation or by energy transfer from the small population of ^{1}*B or ^{1}*A produced by the 400 nm laser pulse is complete well before the $\tau = 60$ ps initial electron-transfer event takes place. The D^+-B^- ion pair recombines with $\tau = 220$ ps, while in D^+-B^--A, the 620 nm B^- band decays, and a 540 nm band appears with $\tau = 140$ ps. The 540 nm band subsequently decays with $\tau = 700$ ns. If the

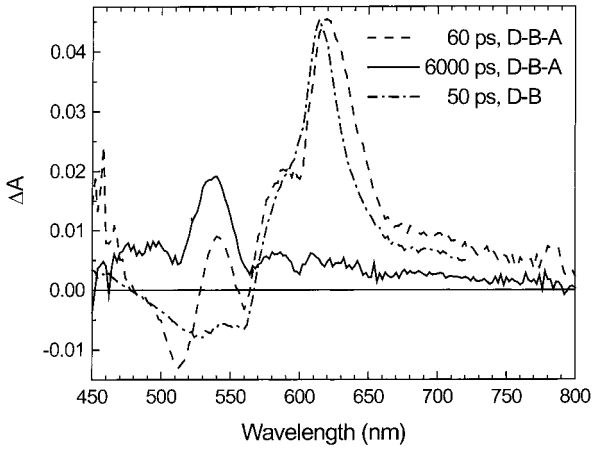

Figure 3. One pump pulse transient absorption spectra of 25 μM D−B−A and D−B in THF at the indicated times following a 130 fs, 400 nm laser pulse.

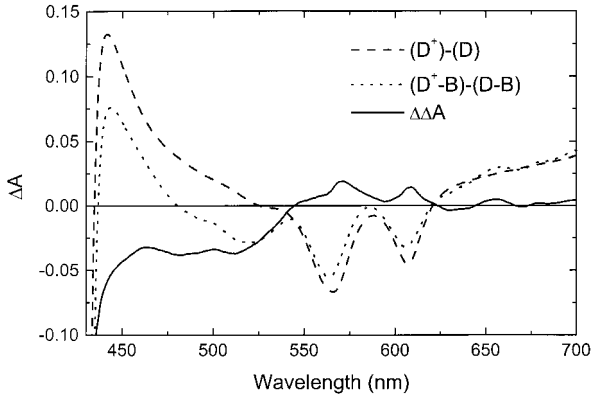

Figure 4. Spectroelectrochemical absorption difference spectra for D^+-B (•••) and D^+(- - -) obtained in *N*,*N*-dimethylformamide containing 0.1 M tetra-*n*-butylammonium hexafluorophosphate. The solid line is the result of subtracting the data for D^+ from that of D^+-B.

540 nm band is due to the formation of D^+-B-A^-, it is difficult to assign because A^- possesses distinct absorption features at 474 nm ($\epsilon = 26000$ M^{-1} cm^{-1}) and 605 nm ($\epsilon = 7200$ M^{-1} cm^{-1}).[24,28]

To understand the origin of the long-lived 540 nm band in the transient absorption spectrum, spectroelectrochemical experiments were carried out on model compounds D, A, D−B, B−A, and B′−A to obtain the spectra of the relevant radical ions. The electric field produced by the presence of D^+ and A^- positioned at a fixed distance on either side of chromophore B within D^+-B-A^- may electrochromically shift the optical absorption of B resulting in the observed 540 nm band.[29] To test this idea, selective one-electron oxidation of D within D−B and reduction of A within B−A were carried out. The difference spectrum $(D^+)-(D)$ in Figure 4 displays a band at 445 nm, as well as bleaches at 560 and 602 nm. This spectrum is typical of the radical cations of other *meso*-substituted zinc porphyrins, such as zinc *meso*-tetraphenylporphyrin, which has a distinct absorption at 445 nm ($\epsilon = 32000$ M^{-1} cm^{-1}) as well as a broad, nearly featureless absorption between 500 and 720 nm (average $\epsilon = 10000$ M^{-1} cm^{-1}).[30] The difference spectrum $(D^+-B)-(D-B)$ in Figure 4 shows that generation of D^+-B also produces a band at 445 nm, as well as bleaches at 517, 560,

(26) The reported distances are center-to-center distances obtained from structures calculated using the MM+ model within Hyperchem by Hypercube, Waterloo, Ontario.

(27) Gosztola, D.; Niemczyk, M. P.; Svec, W. A.; Lukas, A. S.; Wasielewski, M. R. *J. Phys. Chem.* Submitted for publication.

(28) Penneau, J. F.; Stallman, B. J.; Kasai, P. H.; Miller, L. L. *Chem. Mater.* **1991**, *3*, 791−6.

(29) Liptay, W. *Angew. Chem., Int. Ed. Engl.* **1969**, *8*, 177−188.

(30) Fajer, J.; Borg, D. C.; Forman, A.; Dolphin, D.; Felton, R. H. *J. Am. Chem. Soc.* **1970**, *92*, 3451−3459.

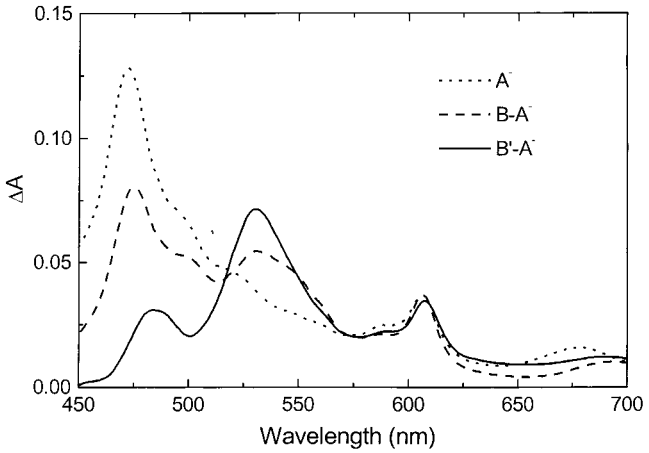

Figure 5. Spectroelectrochemical absorption difference spectra for B−A$^-$(- - -), B′−A$^-$(—), and A$^-$ (•••) obtained in *N*,*N*-dimethylformamide containing 0.1 M tetra-*n*-butylammonium hexafluorophosphate.

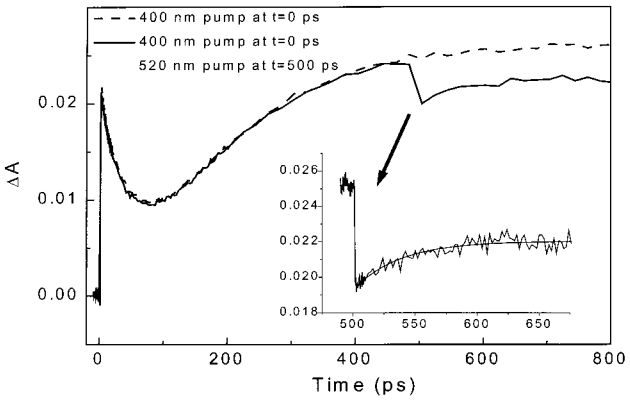

Figure 6. One and two pump pulse transient absorption kinetics of 25 μM D−B−A in THF probed at 540 nm. The inset shows an expansion of the kinetic trace following the second 520 nm pulse at 500 ps.

and 602 nm. Subtracting the difference spectrum (D$^+$)−(D) from that of (D$^+$−B)−(D−B), $\Delta\Delta A$ in Figure 4, shows that the 445, 560, and 602 nm bands are due to the presence of D$^+$, while the effect of D$^+$ on the absorption of B produces the broad bleach at 500 nm and a positive band at 570 nm. Residual features due to the Q-bands of D are superimposed on the 570 nm band. The bandshift of the B absorption due to the presence of D$^+$ is significant even though the ions are generated in polar media. This most likely occurs because direct attachment of D$^+$ to B effectively limits solvent access to the space between D$^+$ and B resulting in diminished screening of the charge by the solvent.

In a similar manner, selective reduction of A within B−A and B′−A yields the differential absorption spectra shown in Figure 5, which are compared to that of A$^-$. The spectra of B−A$^-$ and B′−A$^-$ show the presence of a broad band near 530 nm, as well as the 474 and 605 nm bands characteristic of A$^-$. These spectra are assigned to electrochromic red shifts of the 517 and 509 nm ground-state absorption bands of B and B′, respectively. These shifts produce a new positive absorption near 530 nm and an absorption loss near 475 nm that partially cancels out the band at 474 nm due to A$^-$. This shift is proportional to the strength of the electric field,[29] so that the ~4 Å shorter distance between B′ and A$^-$ in B′−A relative to that in B−A$^-$ results in a larger red shift in B′−A$^-$. Once again the magnitudes of these effects are significant and suggest that the ability of the polar solvent to screen the charge of A$^-$ is diminished by the limited space between B and A. Thus, the spectroelectrochemical data on both D$^+$−B and B−A$^-$ support the assignment of the 540 nm feature in the transient absorption to the electrochromically red-shifted ground-state absorption of the bridge molecule B within D$^+$−B−A$^-$.

Once D$^+$−B−A$^-$ is formed, B, which initially serves as an electron acceptor, then functions as a chromophore as well. Selective excitation of the perylene-3,4-dicarboximide chromophore, B, can be achieved in the mid-visible region of the spectrum. Using the data in Figures 4 and 5, the absorbance of B within D$^+$−B−A$^-$ at 520 nm is about 5 times greater than that of D$^+$ and A$^-$ combined at that wavelength, which results in more than adequate selectivity for the two-pump-pulse experiments described below. Figure 6 shows the transient absorption kinetics at 540 nm for both the single-pulse and two-pulse experiments. In both experiments at $t = 0$, a 400 nm, 130 fs laser pulse (pump 1) initiates the formation of D$^+$−B−A$^-$. The instrument limited absorption increase at $t = 0$ is due to formation of ^{1}*D−B−A, which decays to D$^+$−B$^-$−A with $\tau = 60$ ps. This decay time agrees well with the decay time found for D$^+$−B$^-$−A by selectively monitoring B$^-$ at 620 nm. In addition, the subsequent rise of the signal with $\tau = 140$ ps monitors the formation of D$^+$−B−A$^-$ and agrees well with the time constant found for the decay of D$^+$−B$^-$−A monitored at 620 nm. Thus, at early times kinetics for all of the key intermediates in the formation of D$^+$−B−A$^-$ are observed at 540 nm, while at longer times 540 nm monitors only the presence of D$^+$−B−A$^-$.

At $t = 500$ ps, bridging molecule B within D$^+$−B−A$^-$ is selectively excited with a 520 nm, 150 fs laser pulse (pump 2). Following the 520 nm pulse, the transient absorption kinetics monitored at 540 nm show a sharp decrease in intensity that occurs with the instrument response $\tau = 0.2$ ps, Figure 6 and inset. The magnitude of this decrease is a function of the number of 520 nm photons absorbed by the sample. Disappearance of the 540 nm band monitors the loss of D$^+$−B−A$^-$. After formation of D$^+$−^{1}*B−A$^-$, 45% of the immediate absorption change recovers with $\tau = 50$ ps to a new ΔA value that is 20% less than that which D$^+$−B−A$^-$ displays when B is not photoexcited (Figure 6, dashed curve). The new, lower concentration of D$^+$−B−A$^-$ decays with the expected 700 ns time constant. The ΔA data suggest that D$^+$−^{1}*B−A$^-$ decays by competitive pathways in which about 55% of the population of D$^+$−^{1}*B−A$^-$ leads to D−B−A, while 45% re-forms D$^+$−B−A$^-$.

There are two principal charge recombination pathways leading from D$^+$−^{1}*B−A$^-$ to D−B−A. Following excitation of B, if the reaction D$^+$−^{1}*B−A$^-$ → D$^+$−B$^-$−A ($\Delta G = -2.0$ eV) occurs,[14] then the transient absorption spectrum of D$^+$−B$^-$−A should appear following the 520 nm laser pulse. Subsequently, D$^+$−B−A$^-$ should re-appear with the same τ =140 ps time constant that is observed in the one pulse excitation experiment. Neither of these characteristics is observed. The observation of the $\tau = 50$ ps recovery of the 540 nm band suggests that a different reaction occurs following the formation of D$^+$−^{1}*B−A$^-$. The corresponding hole transfer reaction D$^+$−^{1}*B−A$^-$ → D−B$^+$−A$^-$ ($\Delta G = -1.6$ eV) should be faster than the electron transfer described above because ΔG for the electron transfer is further into the Marcus inverted region than is the hole transfer.[31] If the hole transfer mechanism of charge recombination occurs, it should be possible to observe the loss of D$^+$ and/or the formation of B$^+$ due to the reaction D$^+$−^{1}*B−A$^-$ → D−B$^+$−A$^-$. In addition, the observed $\tau = 50$ ps kinetic component for the recovery of the 540 nm absorption

(31) Marcus, R. A. *J. Chem. Phys.* **1956**, *24*, 966−978.

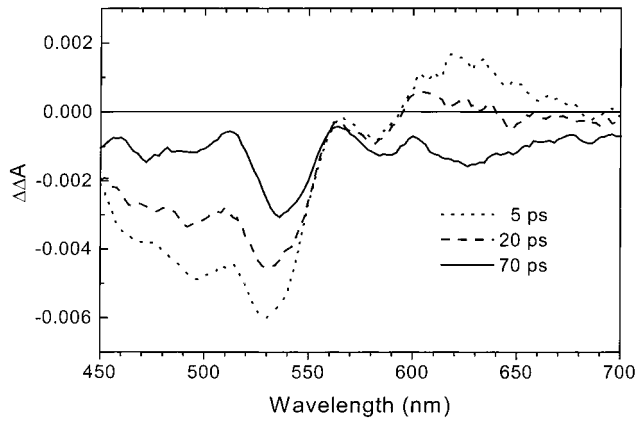

Figure 7. Two pump pulse transient absorption spectra of 25 μM D−B−A in THF following a 400 nm, 130 fs, laser pulse at $t = 0$ ps and a 520 nm, 150 fs, laser pulse at 500 ps. The times given are following the second pump pulse.

(inset, Figure 6) should be approximately the sum of the rate constants for the two reactions:

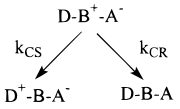

(2)

Figure 7 shows the transient absorption spectra that appear at 5, 20, and 70 ps following the application of the second 520 nm excitation pulse at $t = 500$ ps. The spectrum at 5 ps clearly shows the loss in absorbance at 540 nm that results from formation of $D^+-{}^1*B-A^-$, as well as further loss between 450 and 540 nm, and a modest increase between 590 and 650 nm. A comparison of the spectral changes between 450 and 540 nm with the $(D^+)-(D)$ spectral data in Figure 4 strongly suggests that these changes are consistent with the loss of D^+ that occurs when the reaction of $D^+-{}^1*B-A^- \rightarrow D-B^+-A^-$ takes place. The optical spectrum of B^+ obtained by single 520 nm pulse excitation of B′−A (data not shown) consists of a broad featureless absorption that extends from 530 to 650 nm with a maximum at 580 nm. The small residual absorbance between 590 and 650 nm may be due to the part of the B^+ absorption that is not canceled by the strong bleach between 450 and 540 nm. At 20 ps following both laser flashes, the D^+ signal recovers somewhat, as does the absorption between 590 and 650 nm. These changes are most likely due to the fraction of the $D-B^+-A^-$ population that returns to D^+-B-A^-. Finally, a comparison between the transient spectrum of D^+-B-A^- generated using a single 400 nm laser flash, Figure 3, with that at 70 ps following two sequential laser flashes at 400 and 520 nm, Figure 7, shows that the spectra are nearly identical throughout the measured wavelength range. The only significant difference between them is the fact that the spectrum in Figure 7 shows an overall loss in D^+-B-A^- population following both laser flashes.

Transient absorption spectroscopy following excitation of B−A with a single 520 nm laser pulse shows that $\tau = 100$ ps for the reaction $B^+-A^- \rightarrow B-A$ (data not shown). Thus, referring to eq 2, $1/\tau = k_{CS} + k_{CR}$, where $k_{CR} = 1.0 \times 10^{10}$ s^{-1} and $1/\tau = 2.0 \times 10^{10}$ s^{-1}, thus $k_{CS} = 1.0 \times 10^{10}$ s^{-1}. The kinetic data suggest that about half of the $D-B^+-A^-$ population decays by each pathway. This agrees well with the observed amplitudes of the absorbance changes depicted in the inset to Figure 6, where 55% of the initial population of $D^+-{}^1*B-A^-$ yields D−B−A, while 45% yields D^+-B-A^-. Considering that the rate-limiting step for charge recombination is the reaction $D-B^+-A^- \rightarrow D-B-A$, application of the second laser pulse increases the charge recombination rate by a factor of 7000 over the 1.4×10^6 s^{-1} natural rate constant for D^+-B-A^- recombination.

Conclusions

This work shows that it is possible to significantly change the electron transfer dynamics within a donor−bridge−acceptor system by changing the electronic state of the bridge molecule. Photoexcitation of the bridging molecule results in partially occupied orbitals that can interact strongly with those of the adjacent donor and acceptor. We are exploring photonic control of charge transmission in a variety of related systems to probe fundamental issues regarding the ability of organic molecules to exhibit photoswitchable wire-like behavior.

Experimental Section

Compounds D−B−A, D−B, B−A, and B′−A were synthesized using methods described in the Supporting Information section. The syntheses of D and A were described previously.[23] The structures of these compounds were confirmed using ^{1}H NMR and mass spectral data.

Electrochemistry and Spectroelectrochemistry. Cyclic voltammetry (CV) and bulk electrolysis were carried out using a computer controlled potentiostat (Princeton Applied Research, Model 273, M270 software package) and a standard three-electrode arrangement. CV measurements used both platinum working and auxiliary electrodes and a saturated sodium calomel reference electrode (SSCE). All electrochemical measurements were carried out in N_2 purged DMF or butyronitrile with 0.1 M Bu_4NPF_6 as the supporting electrolyte. The scan rate for CV measurements was typically 50−100 mV/s. Ferrocene was used as an internal redox standard for all potentiometric measurements. Spectroelectrochemistry of D−B, B−A, B′−A, D, and A each dissolved in N_2 purged *N*,*N*-dimethylformamide containing 0.1 M tetra-*n*-butylammonium hexafluorophosphate was carried out in an optically transparent thin layer electrochemical cell using a 2 cm^2, 250 lines/in. gold minigrid electrode.[32,33] Controlled potential oxidation of D at 1.0 V vs SCE was used to generate D^+, while controlled potential reduction of A at −0.7 V vs SCE was used to generate A^-. These over-potentials are required to overcome the internal resistance of the cell. Returning the potentials back to 0 V vs SCE restored the initial optical spectra. Ground-state optical absorption measurements of the neutral and radical ion species were recorded using a computer-controlled spectrophotometer (Shimadzu, Model 1601), and the differential absorption spectrum (ΔA) was calculated by subtracting the ground-state spectrum from that of the radical ion.

Transient Spectroscopy. Femtosecond transient absorption measurements were obtained with pump wavelengths of 400 nm, 520 nm, or both and a white light continuum probe pulse produced by an amplified-Ti:sapphire laser system with an optical parametric amplifier (OPA) as described previously.[15] The total instrument function is 180 fs. The concentrations of samples of D−B−A, D−B, and B−A used for transient absorption measurements were approximately 25 μM in 2 mm path length cells. Both pump beams and the probe beam were 200 mm in diameter with the 400 and 520 nm pump beams having energies of 2 and 1 μJ at the sample, respectively.

Acknowledgment. This work was supported by the National Science Foundation (CHE-9732840).

Supporting Information Available: Preparation and characterization of D−B−A, D−B, B−A, B′−A, and B (PDF). This material is available free of charge via the Internet at http://pubs.acs.org.

JA000219D

(32) Murray, R. W.; Heineman, W. R.; O'Dom, G. W. *Anal. Chem.* **1967**, *39*, 1666−8.

(33) DeAngelis, T. P.; Heineman, W. R. *J. Chem. Educ.* **1976**, *53*, 594−597.